5th US Combustion Meeting
Organized by the Western States Section of the Combustion Institute
and Hosted by the University of California at San Diego
March 25-28, 2007.

Direct numerical simulation of stationary lean premixed methane-air flames under intense turbulence

Ramanan Sankaran[1], Evatt R. Hawkes[2], Chun S. Yoo[2], Jacqueline H. Chen[2], Tianfeng Lu[3] and Chung K Law[3]

[1]*National Center for Computational Sciences, Oak Ridge National Laboratory, Oak Ridge, TN 37831-6008*

[2]*Combustion Research Facility, Sandia National Laboratories, Livermore, CA 94551-0969*

[3]*Department of Mechanical and Aerospace Engineering, Princeton University, Princeton, NJ 08540-5263*

Direct numerical simulation of a three-dimensional spatially-developing turbulent Bunsen flame has been performed at three different turbulence intensities. The simulations are performed using a reduced methane-air chemical mechanism which is specifically tailored for the lean premixed conditions simulated here. A planar-jet turbulent Bunsen flame configuration is used in which turbulent preheated methane-air mixture at 0.7 equivalence ratio issues through a central jet and is surrounded by a hot laminar coflow of burned products. The turbulence characteristics at the jet inflow are selected such that combustion occurs in the thin reaction zones (TRZ) regime. At the lowest turbulence intensity the conditions fall on the boundary between the TRZ regime and the corrugated flamelet regime. At the highest turbulence intensity the conditions correspond to the boundary between the TRZ regime and the broken reaction zones regime. The data from the three simulations is analyzed to understand the effect of turbulent stirring on the flame structure and thickness. Statistical analysis of the data shows that the thermal preheat layer of the flame is thickened due to the action of turbulence, but the reaction zone is not significantly affected.

1 Introduction

Premixed combustion under intense turbulence is of fundamental interest due to its relevance to practical applications such as lean premixed stationary gas turbines. Premixed flames under lean conditions tend to be thicker, propagate slower and the flame structure is more susceptible to the influence of turbulence. Recently, Peters [1] has provided a model for flame propagation in the regime where the turbulence scales are capable of penetrating and influencing the preheat zone, but are incapable of penetrating the reaction zones. This regime is called the thin reaction zones (TRZ) regime.

Premixed flame structure consists of a broader preheat layer upstream of a narrower reaction layer. Usual modeling approaches for the TRZ regime assume that the turbulent eddies can enter and influence the preheat layer - but the reaction zone, being thinner than the preheat layer by an

order of magnitude, is not penetrated. The assumption of an order of magnitude disparity in the thickness of the preheat layer versus the reaction layer is based on theoretical analysis of the flame structure using activation energy asymptotics. In practical fuels such as methane-air, especially at lean conditions, the preheat layer is only three times wider than the reaction layer, approximately. It needs to be determined if the reaction layer indeed stays intact in the TRZ regime despite the fact that it is not as thin as commonly assumed.

It is also not clear whether the flame dynamics in this regime are dominated by the entrainment of small eddies into the flame structure or the large scale flow straining which does not alter the flame structure. The penetration of the local flame structure by small eddies is expected to cause thickened flames in the TRZ regime [1, 2]. However the competetive effect of the large scale structure is expected to thin the flame. Thus, it unclear whether flames are thicker or thinner in the TRZ regime. Several experimental studies in this regime have reported [3, 4] thicker flames, while others have reported thinner flames [5, 6]. Computations have also not yet delivered a definitive result. One-dimensional Linear Eddy Model computations [7] show thickened flames and three-dimensional direct numerical simulation [8] show there is some probability of encountering thicker flames, but more likely flames are thinner. Two-dimensional decaying turbulence simulations [9] and three-dimensional expanding flame simulations [10] found that, on average, the flame gets thinner. These results, not only contradict the common theoretical description of the flame structure [2], but are also inconclusive due to the lack of realism in two-dimensional turbulence and lack of statistical stationarity in the expanding flame configuration.

Here, 3D fully-resolved direct numerical simulations (DNS) of turbulent premixed combustion are performed in a spatially-developing slot-burner Bunsen flame configuration with a detailed methane-air chemical mechanism. So far, three simulations in the TRZ regime at successively higher turbulence intensities have been performed as part of a parametric study. The data is analyzed to obtain statistical measures of the influence of turbulence on flame structure. In particular the effect of turbulent strain on preheat layer thickness and the integrity of the reaction layers are studied.

2 Problem Configuration

The simulation was performed in a slot-burner Bunsen flame configuration. The slot-burner Bunsen configuration is especially interesting due to the presence of mean shear in the flow and is similar in configuration to the burner used in experimental studies, for example by Filatyev *et al.* [11]. This configuration consists of a central reactant jet through which premixed reactants are supplied. The central jet is surrounded on either side by a heated coflow, whose composition and temperature are those of the complete combustion products of the reactant jet. This arrangement is similar to the pilot flame surrounding slot burners commonly used in experiments [11]. The reactant jet was chosen to be a premixed methane-air jet at 800K and ϕ = 0.7. The unstrained laminar flame properties at these conditions computed using PREMIX [12] are as follows:

1. Flame speed, S_{L} = 1.8 m/s
2. Thermal thickness based on maximum temperature gradient, δ_{L}=0.3mm
3. Full width at half maximum (FWHM) of heat release rate, δ_{H} = 0.14mm, and

4. Flame time scale, $\tau_{\rm f}$=$\delta_{\rm L}/S_{\rm L}$=0.17ms.

One of the reasons for choosing a preheated inflow condition is that the cost of computation is inversely proportional to the Mach number at the inflow. Preheating the reactants leads to a higher flame speed and allows a higher inflow velocity without blowing out the flame. Also, many practical devices such as internal combustion engines, gas turbines and recirculating furnaces operate at highly preheated conditions. One important consequence of preheating is that the reaction zone is broadened at 800K ($\delta_{\rm L}/\delta_{\rm H}$=2) compared to 300K ($\delta_{\rm L}/\delta_{\rm H}$=3). However, the preheat temperature chosen here is low enough that flameless combustion [13] does not occur.

A parametric study was performed to investigate the effect of increasing turbulence intensity on lean premixed combustion. The problem configuration, mixture equivalence ratio and temperature are the same for all three simulations. However, they differ in the domain sizes and inflow turbulence conditions. The simulation parameters are given in Table 1. A uniform grid spacing of 20μm was used in the streamwise, x, and spanwise, z, directions, while an algebraically stretched mesh in the transverse,y, direction was obtained from $y(s) = f(s) \times s$, where s is the equi-spaced computational grid and $0 \leq s \leq 1$. The stretching function is given by,

$$f(s) = \beta s + \frac{1}{2}\left(1 + \tanh\frac{s - s^*}{\sigma}\right)\left(e^{ks} - \beta s\right), \tag{1}$$

where $k = \ln(\beta s^*)/(s^* - 1)$. The resultant mesh was mirrored across the jet centerline ($y = s = 0$) to obtain a symmetric mesh. The form of the stretching function along with the choice of constants, $\beta = 0.55$, $s^* = 0.75$ and $\sigma = 1/16$, yields a mesh that has a uniform spacing of 20μm in the center of the domain over a region $5h$ in width. Here h denotes the slot width. The increase in grid spacing, $(\Delta_{i+1}/\Delta_i - 1)$, in the outer part of the domain does not exceed 2%. While the uniform grid spacing at the center of the jet ensures numerical fidelity and flexibility in post-processing, the boundaries are pushed farther away to reduce their influence on the flame.

Numerical Method

A reduced chemical mechanism for lean premixed methane-air flames was derived, specifically tailored to minimize temporal stiffness while maintaining accuracy. The reduction was accomplished through the sequential application of directed relation graph (DRG), sensitivity analysis and computational singular perturbation (CSP) over the GRI-1.2 detailed mechanism. Details on the reduction methodology and validation of the reduced mechanism can be found in Ref. [14, 15]. A notable aspect of the reduced mechanism is that the quasi-steady state (QSS) species concentrations were obtained through explicit analytical expressions without the need for expensive iterations. Consequently, overall convergence was obtained at a lower cost.

The simulations were performed using the DNS code S3D, which solves the fully compressible Navier Stokes, species and energy equations with a fourth-order Runge-Kutta method for time integration and an eighth-order explicit spatial differencing scheme [16, 17]. A tenth-order filter was used periodically to damp any spurious high-wave number oscillations. The mixture specific heat is determined locally as a function of mixture composition; that is, $C_p = \sum_k C_{p,k} Y_k$, where each $C_{p,k}$ is curve-fitted as a function of temperature using the Chemkin thermodynamic database [18].

Table 1: Simulation parameters

	Case A	**Case B**	**Case C**
slot width (h)	1.2mm	1.2mm	1.8mm
Domain size in the streamwise, crosswise and spanwise directions	$12h \times 12h \times 3h$	$20h \times 12h \times 3h$	$20h \times 12h \times 3h$
Number of grid points	52 Million	88 Million	195 Million
Turbulent jet velocity ($\bar{U}$)	60m/s	100m/s	100m/s
Laminar coflow velocity	15 m/s	25 m/s	25 m/s
Jet Reynolds number ($\mathrm{Re}_{\mathrm{jet}} = \bar{U}h/\nu$)	840	1400	2100
Turbulence intensity[4] (u'/S_{L})	3	6	10
Turbulence length scale[2,4] ($l_{\mathrm{t}}/\delta_{\mathrm{L}}$)	0.7	1	1.5
Integral length scale[3,4] ($l_{33}/\delta_{\mathrm{L}}$)	2	2	4
Turbulence Reynolds number($\mathrm{Re}_{\mathrm{t}} = u' l_{33}/\nu$)	40	75	250
Karlovitz Number $(\delta_{\mathrm{L}}/l_{\mathrm{k}})^2$	100	100	225

[1] Kinematic viscosity at the inflow conditions, $\nu = 8.5e-5m^2/s$, is used to compute Reynolds number.
[2] Turbulence length scale l_{t} is estimated as $l_{\mathrm{t}} = u'^3/\tilde{\epsilon}$, where $\tilde{\epsilon}$ is the average turbulent kinetic energy dissipation rate.
[3] Integral length scale l_{33} is defined as the integral of the auto-correlation of the spanwise component of velocity in the spanwise direction.
[4] The turbulence scales evolve from the synthetic turbulence specified at the inflow. The u', l_{t} and l_{33} values reported here are at the 1/4th streamwise location along the jet centerline.

The molecular viscosity is also temperature dependent and constant Lewis numbers for individual species are used.

The flame is anchored at the inflow plane by specifying the species mass fractions and temperature from an unstrained laminar flame solution using a progress variable lookup. A hyperbolic tangent function was used to obtain a smooth variation of progress variable between the unburned and burned conditions. A turbulent velocity field was synthesized by specifying the length scale, magnitude of velocity fluctuations and spectral energy density. The resultant velocity field was added to the mean inflow velocity profile and used as the velocity inflow boundary condition based on Taylor's hypothesis.

Navier-Stokes characteristic boundary conditions (NSCBC) [19–22] were used to prescribe the boundary conditions. The boundary conditions were periodic in the spanwise direction (z), non-reflecting inflow and outflow in the streamwise direction (x), and non-reflecting outflow [19] in the transverse direction (y). Based on the jet inlet velocity and the streamwise domain length, a flow-through time is 0.24ms. The solution was advanced at a constant 2ns time-step for three flow through times for case A and two flow through times for cases B and C. The first flow through time was neglected to account for initial transients when performing analysis. Data from 61 equally spaced time instants from the remainder of the simulation was used to obtain the statistical results presented in the next section. Averaging is performed in the homogeneous direction (z) and time. Symmetry across the centerline is exploited where feasible.

3 Results and Discussion

A reaction progress variable, c, is defined based on the mass fraction of O_2. While c is usually defined based on the deficient reactant, in this case CH_4, such a definition here will omit a significant portion of the oxidation layer, since the heat release is only 66% complete where CH_4 is completely consumed. Therefore, c is defined using O_2 mass fraction. Based on the laminar flame solution at the chosen reactant conditions, the heat release is a maximum at c = 0.65. Therefore, the iso-surface corresponding to c = 0.65 is taken as the flame surface. The mean progress variable computed by favre-averaging is shown in Fig. 1.

Figure 2 shows the instantaneous flame surface for the three cases. In all three cases the flame is initially planar at the inlet, but is wrinkled within a short distance in the downstream direction. Also the scale of wrinkling increases in the downstream direction. Comparing the three cases, it is seen that the amount of wrinkling increases from case A to case C. Also there is a significantly higher amount of flame-flame interaction in cases B and C compared to case A. The flame-flame interaction leads to pinch-off as evident in the far downstream location in case A. This effect is more pronounced in cases B and C where the pinch-off is noticed further upstream. In case C, the pinch-off and mutual annihilation of flame surface due to interaction are found to occur even at locations very close to the jet inlet. This shows that the flame-flame interaction is a dominant mechanism limiting the flame surface area generated by wrinkling due to turbulence. Another interesting observation is that the shape of the flame is mostly convex towards the products and forms sharper cusps towards the reactants. This is contrary to the expected behavior for a Huygens-type self propagation and is evidence that the flame topology is strongly influenced by turbulent straining.

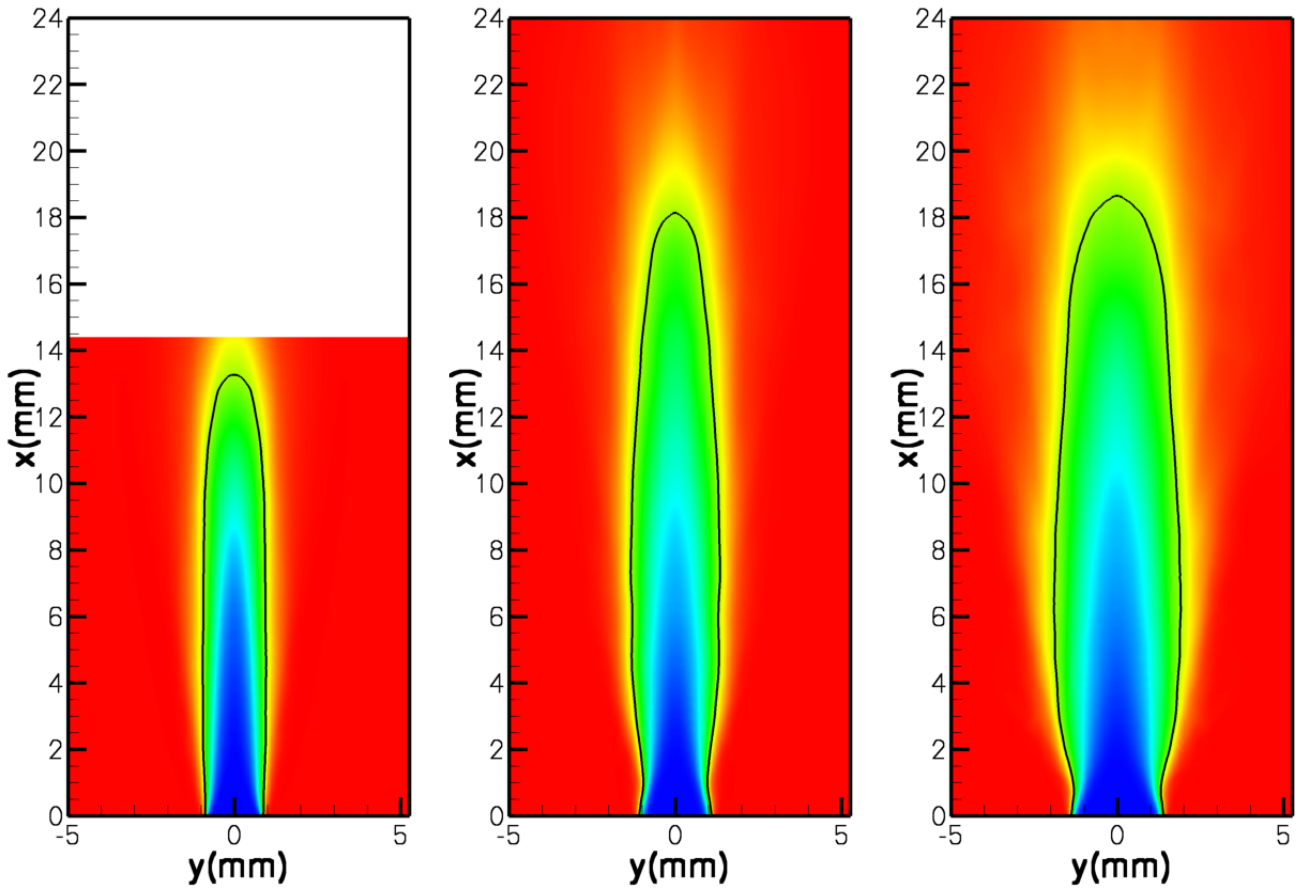

Figure 1: Favre averaged mean progress variable ($\tilde{c}$) is shown as a pseudocolor plot. The color scale varies from blue (0) to red (1). The iso-contour of $\tilde{c} = 0.65$ is shown as a solid line.

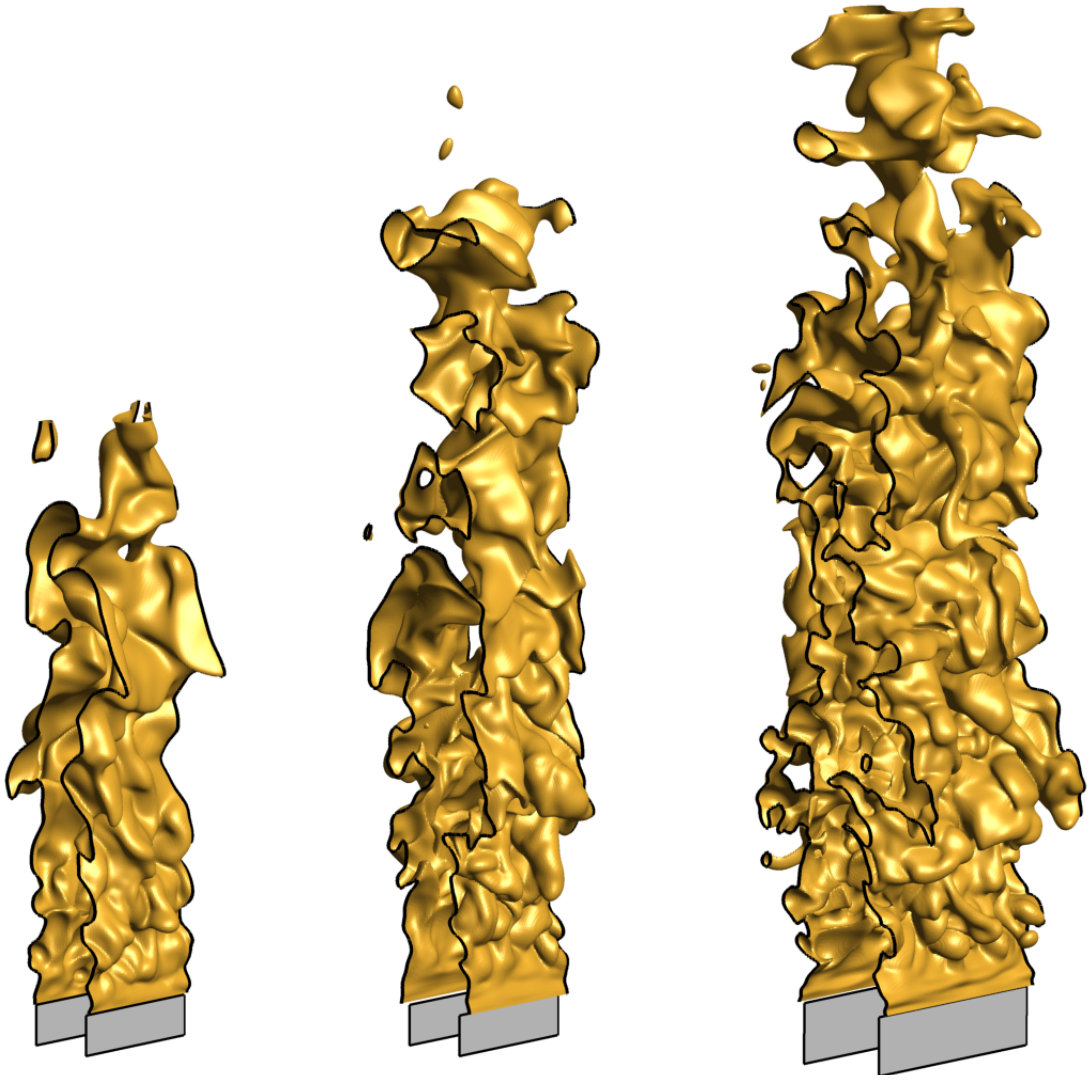

Figure 2: Instantaneous iso-contour of the progress variable ($c = 0.65$) representing flame surface for cases A, B and C.

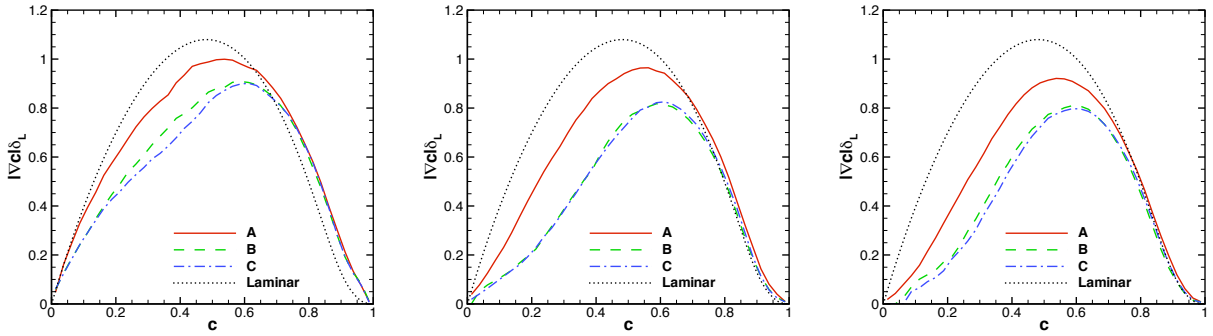

Figure 3: Conditional means of $|\nabla c|$ compared to the laminar flame profile for the three simulations. The means are computed at three chosen streamwise locations corresponding to 1/4, 1/2 and 3/4th of the domain length in the stream-wise direction.

3.1 Effect on flame thickness

As mentioned in the introduction, the effect of turbulent stirring on the flame thickness in the TRZ regime is not clearly understood. Here, the data from the DNS is analyzed to determine if, on average, the flame thickness increases or decreases relative to a laminar flame. The reciprocal of the magnitude of progress variable gradient, $1/|\nabla c|$ yields a flame thickness analogous to the definition used for the laminar thermal thickness δ_{L}. $|\nabla c|$ is averaged over intervals of c and compared with the unstrained laminar flame profile in Fig. 3. In ref. [15], the conditional mean of $|\nabla c|$ was presented for case A and the results showed that the mean $|\nabla c|$ was lower in the turbulent flame than in a laminar flame, which indicated flame thickening. Here, the same analysis is also applied to cases B and C, to verify if the flame continues to get thicker as the turbulence intensity is increased. A comparison of case A with case B in Fig. 3 shows that the mean gradients are further reduced. This again indicates an increase in flame thickening due to the increase in turbulence intensity from u'/S_{L} = 3 to 6. However, a comparison of case B with case C shows that there is negligible increase in flame thickness even though the turbulence intensity was increased from u'/S_{L} = 6 to 10. This is a very interesting result and shows that any further increase in turbulence intensity beyond a threshold level does not result in thicker flames.

The thickening of the flame is further validated using additional analysis methods. A distance function D is defined such that at every point in the domain the quantity D is the shortest normal distance from the flame-surface [23, 24]. The distance function is computed by solving the Eikonal equation,

$$|\nabla D| = 1 \tag{2}$$

subject to the boundary condition $D = 0$ on the flame surface. The flame surface is defined as the isosurface $c = 0.65$ and the distance to this surface, D, is computed. The distance is defined as negative in the fresh gas side and positive in the burned gas side. An illustration of the distance function versus the progress variable iso-surface is shown in Fig. 4. The figure shows a slice perpendicular to the streamwise direction. The progress variable is shown in color and the iso-contours of the computed distance function are shown as line contours. The distance function iso-contours represent the locus of all points that are equidistant from the flame surface, $D = 0$.

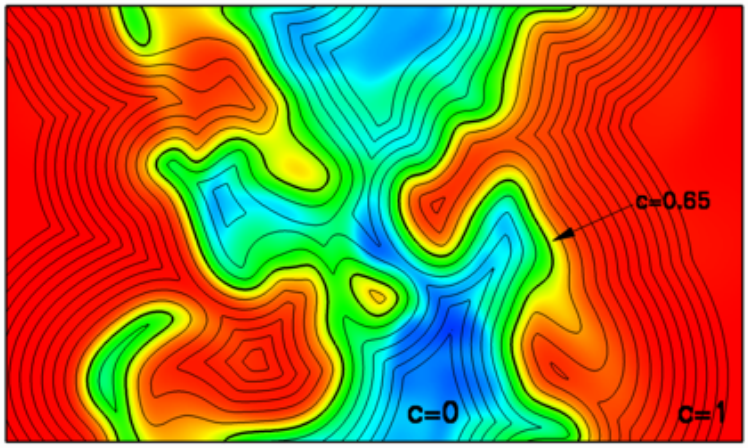

Figure 4: Progress variable (c) and distance function (D) are shown in a slice of the domain perpendicular to the streamwise direction. c is shown in color on a blue (c=0) to red (c=1) scale. The lines represent iso-contours of D. The darkest iso-contour line represents $D = 0$, which also corresponds to the iso-contour of $c = 0.65$.

Where the flame surface is curved, the distance function is discontinuous on the center of curvature side and has a ridge-like appearance. The ridge is the locus of all points that are equidistant from multiple points on the flame surface [23].

Here, the effect of turbulence on the flame structure is analyzed by obtaining statistical means conditional on the distance from the flame surface. Figure 5 shows the mean and standard deviation of temperature and O_2 mass fraction as a function of the distance function for cases A, B and C at the '1/2' streamwise location. Since the progress variable, c, is defined based on O_2 mass fraction, the figures are also indicative of the mean and standard deviation of c. It is seen from the mean temperature profile that the preheat layer of the flame is significantly thickened. The mean temperature ahead of the flame is higher indicating that there is an enhanced activity in the preheat layer leading to an increased amount of heat diffusion into the unburnt gas region. This is also evident from the mean O_2 mass fraction profiles, where O_2 is depleted in the preheat layer due to its transport into the reaction zone. However comparing cases B and C, no significant difference is seen in the mean profiles. This is in agreement with the finding based on Fig. 3 that the higher turbulence intensity in case C compared to case B did not further increase the mean flame thickness.

Figure 5 also shows the standard deviation of temperature and O_2 mass fraction for the three cases. It should be noted that since the distance is computed from the Y_{O2} iso-surface, the standard deviation of Y_{O2} is zero at $D = 0$ by definition. O_2 mass fraction is strongly correlated with temperature and therefore the standard deviation of temperature is also very low near $D = 0$. Therefore, the dip seen in the standard deviations of temperature and Y_{O2} is not an anomaly. Instead, it is a consequence of the definition used for the flame surface and is expected. However, ahead in the fresh gas region a comparison of the standard deviations among the three cases provides very useful information. It is seen that the standard deviation increases with turbulence intensity. It is also seen that comparing cases B and C there is a small increase in the level of fluctuations. This suggests that while the mean profiles are similar for cases B and C, differences appear in higher moments.

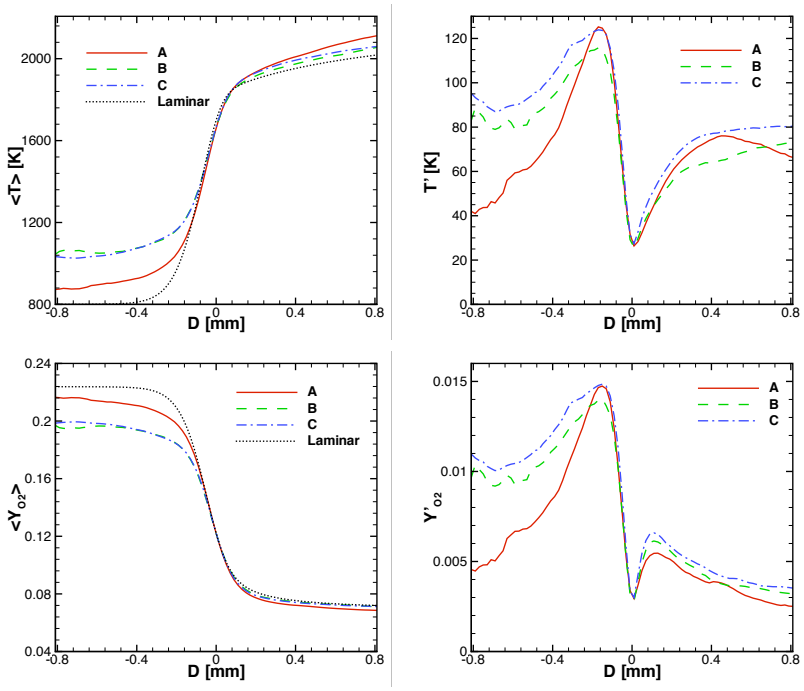

Figure 5: Mean and standard deviation of temperature and Y_{O2} conditional on the distance from the flame surface. Means are computed at the streamwise location '1/2'.

3.2 Effect on reaction layer

In Ref. [15], the mean reaction rates conditional on the progress variable were compared to the laminar reaction rate profiles to study the influence of turbulence on the reaction zone structure. Here we extend the analysis to cases B and C. Also, instead of using c as the conditioning variable, we use the distance variable D to obtain conditional mean reaction rate profiles. Figure 6 shows the mean heat release rate profile and mean reaction rate profiles for CH_4 and OH. The three cases A, B and C show excellent agreement with each other. There is some difference between the magnitudes of the mean reaction rates and the laminar profile. This difference may be reduced by comparison with the reaction rates corresponding to a strained laminar flame rather than a freely propagating laminar flame. The location and width of the different reaction layers agree well with the laminar flame. This again confirms the hypothesis [1] that turbulence does not have a significant influence on the reaction zone even in the TRZ regime. Although the reaction zone here is not really 'thin' (δ_L/δ_H), the lack of significant influence on the reaction layer can possibly be the result of the dissipation of turbulence due to heat release. This is the subject of an ongoing investigation.

4 Concluding Remarks

Three-dimensional direct numerical simulation of a spatially-developing slot Bunsen flame was simulated at three successively higher turbulence intensities. The data was analyzed to study the interaction of turbulence and chemistry in the thin reaction zones regime of combustion. Using

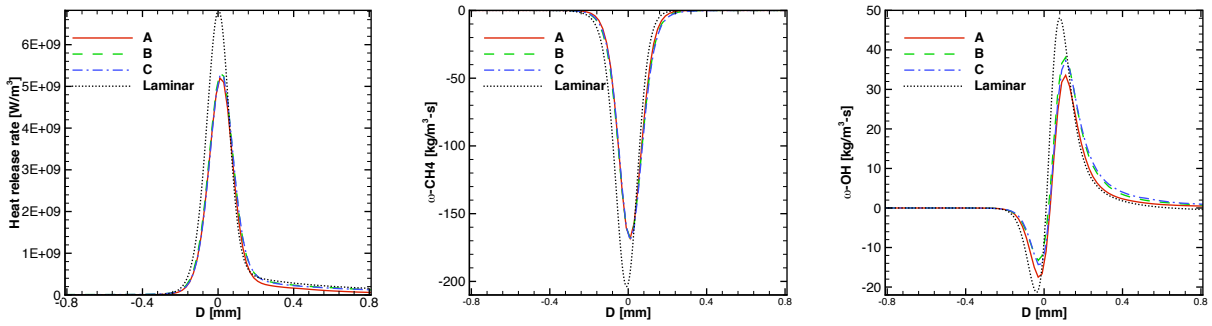

Figure 6: Mean heat release rate and reaction rates conditional on the distance from the flame surface compared to the laminar profile.

statistical measures, it was found that turbulence thickens the preheat layer of the flame. However beyond a certain level, further increase in turbulence intensity does not alter the mean thickness of the flame. A higher probability of flame interaction and annihilation at the higher turbulence intensities is one possible reason for the lack of any further thickening when the turbulence intensity is increased beyond a certain level. The structure of the reaction zone and heat release layer is analyzed by obtaining mean reaction rates conditional on a distance function. The results show that there is no influence on the reaction zones and they remain unperturbed for all of the cases considered.

Acknowledgments

The work at SNL was supported by the Division of Chemical Sciences, Geosciences and Biosciences, the Office of Basic Energy Sciences (BES), the U.S. Department of Energy (DOE) and also by the U.S. DOE, BES, SciDAC Computational Chemistry program. SNL is a multiprogram laboratory operated by Sandia Corporation, a Lockheed Martin Company, for the U.S. DOE under contract DE-AC04-94-AL85000. The work at Princeton was supported by the Air Force Office of Scientific Research under the technical monitoring of Dr. Julian M. Tishkoff. The work at ORNL was supported by and this research used resources of the National Center for Computational Sciences (NCCS) at Oak Ridge National Laboratory (ORNL), which is supported by the Office of Science of the U.S. DOE under Contract No. DE-AC05-00OR22725.

References

[1] N. Peters. *Journal of Fluid Mechanics*, 384 (1999) 107–132.

[2] N. Peters. *Turbulent Combustion*. Cambridge university press, New York, 2000.

[3] M. S. Mansour, N. Peters, and Y. C. Chen. *Proceedings of the Combustion Institute*, 27 (1998) 767–773.

[4] Y. C. Chen and M. S. Mansour. *Proceedings of the Combustion Institute*, 27 (1998) 811–818.

[5] F. Dinkelacker, A. Soika, D. Most, D. Hofmann, A. Leipertz, W. Polifke, and K. Dobbeling. *Proceedings of the Combustion Institute*, 27 (1998) 857–865.

[6] A. Soika, F. Dinkelacker, and A. Leipertz. *Proceedings of the Combustion Institute*, 27 (1998) 785–792.

[7] V. Sankaran and S. Menon. *Proceedings of the Combustion Institute*, 28 (2000) 203–209.

[8] M. Tanahashi, Y. Nada, Y. Ito, and T. Miyauchi. *Proceedings of the Combustion Institute*, 29 (2002) 2041–2049.

[9] E. R. Hawkes and J. H. Chen. Direct numerical simulation of premixed flames in the thin reaction zones regime. In *Proceedings of the 2003 Winter Meeting of the Western States Section of the Combustion Institute*, 2003. Paper no. 03F-68.

[10] D. Thevenin. *Proceedings of the Combustion Institute*, 30 (2005) 629–637.

[11] S. A. Filatyev, J. F. Driscoll, C. D. Carter, and J. M. Donbar. *Combustion and Flame*, 141 (2005) 1–21.

[12] R. J. Kee, J. F. Grcar, M. D. Smooke, and J. A. Miller. PREMIX: A fortran program for modeling steady laminar one-dimensional premixed flames. Technical Report SAND85-8240, Sandia National Laboratories, 1985.

[13] T. Plessing, N. Peters, and J. G. Wunning. *Proceedings of the Combustion Institute*, 27 (1998) 3197–3204.

[14] R. Sankaran, E. R. Hawkes, J. H. Chen, T. Lu, and C. K. Law. Study of turbulent premixed flame thickness using direct numerical simulations in a slot burner configuration. In *Proceedings of the 44nd Aerospace Sciences Meeting and Exhibit, Reno, USA*, 2006. AIAA Paper 2006-0165.

[15] R. Sankaran, E. R. Hawkes, J. H. Chen, T. Lu, and C. K. Law. *Proceedings of the Combustion Institute*, 31 (2007) 1291–1298.

[16] C. A. Kennedy and M. H. Carpenter. *Applied Numerical Mathematics*, 14 (1994) 367–458.

[17] C. A. Kennedy, M. H. Carpenter, and R. M. Lewis. *Applied Numerical Mathematics*, 35 (2000) 177–264.

[18] R. J. Kee, F. M. Rupley, and J. A. Miller. Chemkin-II: A fortran chemical kinetics package for the analysis of gas-phase chemical kinetics. Technical Report SAND89-8009B, Sandia National Laboratories, 1991.

[19] T. J. Poinsot and S. K. Lele. *Journal of Computational Physics*, 101 (1992) 104–129.

[20] J. C. Sutherland and C. A. Kennedy. *Journal of Computational Physics*, 191 (2003) 502–524.

[21] C. S. Yoo, Y. Wang, A. Trouve, and H. G. Im. *Combustion Theory and Modelling*, 9 (2005) 617–646.

[22] C. S. Yoo and H. G. Im. *Combustion Theory and Modelling*, 11 (2007) 259–286.

[23] J. A. Sethian. *SIAM Review*, 41 (1999) 199–235.

[24] T. Deschamps and L. D. Cohen. *Medical Image Analysis*, 5 (2001) 281–299.